PHYSICAL REVIEW B VOLUME 25, NUMBER 2 15 JANUARY 1982

Pressure-optical studies of GeS_2 glasses and crystals: Implications for network topology

B. A. Weinstein, R. Zallen, and M. L. Slade
Xerox Webster Research Center, Webster, New York 14580

J. C. Mikkelsen, Jr.
Xerox Palo Alto Research Center, Palo Alto, California 94304
(Received 17 August 1981)

Germanium disulfide exhibits three solid forms: an amorphous form (a-GeS_2), a layer-structure crystalline form (2D-GeS_2), and a quartzlike crystalline form (3D-GeS_2). We have carried out a series of experiments to determine the effect of pressure on the optical-absorption edge and the near-infrared refractive index of all three forms. We find that pressure causes the absorption edge to red-shift and the refractive index to increase, the sensitivity to pressure being greatest for a-GeS_2, less for 2D-GeS_2, and least for 3D-GeS_2. The size of the initial effect of pressure on the band gap of a-GeS_2 (-23 meV/kbar) is among the largest known for any semiconductor. Analysis of our pressure-optical data for all three forms, taken together with a recently established correlation between covalent-network dimensionality and photoelastic response, leads us to conclude that a-GeS_2 is *not* a 3D-network glass akin to silica, but instead has lower network dimensionality. This is consistent with a class of molecular-glass models such as the Flory model for 1D-network glasses and the Phillips "partially polymerized cluster" model.

I. INTRODUCTION

An essential attribute of amorphous solids is, of course, the absence of long-range order. On the other hand, amorphous materials generally possess short-range order similar to their crystalline analogs of the same chemical composition. The question of the nature and spatial extent of medium-range order is then an important structural issue that must be decided on the basis of a variety of evidence. Recent theoretical work by Phillips has emphasized the topological aspects of short- and medium-range order in covalently-bonded Ge-As-(S,Se) glasses.[1] In an appealingly simple argument based on algebraic topology ideas, he argues that amorphous $Ge_{0.16}(S,Se)_{0.84}$, and $As_2(S,Se)_3$ are superb glass formers because their compositions are such that the average number of force-field constraints per atom exactly exhausts the available spatial degrees of freedom. Phillips also proposes specific structural models for a-$Ge(S,Se)_2$ and a-$As_2(S,Se)_3$ based on reconstructed units derived from the crystalline forms.

In the present work we discuss the structural topology of a-GeS_2 in terms of the useful concept of network dimensionality.[2] By this we mean the number of dimensions in which the covalently-bonded molecular unit is *macroscopically extended.* Examples of crystalline solids with different network dimensionalities are tetrahedral Si (3D network), layer-structure As_2S_3 (2D network), chain-structure trigonal Se (1D network), and orthorhombic S (0D network, consisting of isolated S_8 rings which are finite on an atomic scale and hence macroscopic in *no* dimensions). The last three materials are all molecular solids in which the disconnected molecular units (macromolecular for c-As_2S_3 and c-Se) are formed by and have the dimensional extent of their respective covalent networks. In contrast, c-Si is not a molecular solid since there is no molecular unit which can be "dissected out" (without breaking bonds) of the fully connected covalent network. The point to be emphasized here is that a molecular solid is always characterized by a network dimensionality less than three.

The distinction between molecular and nonmolecular materials on the basis of network dimensionality applies equally well to amorphous solids. Thus, the Polk model of a-Si constitutes a 3D-

network (nonmolecular) structure, as does the atomic arrangement of silica (SiO_2), while the tangled chain (spaghetti-like) model of *a*-Se describes a 1D-network molecular structure. These examples are prototypical of two classic models for topological disorder in covalent glasses: Zachariasen's continuous-random-network model,[3] and Flory's random-coil polymer model.[4] Figure 1 illustrates these contrasting models. The Flory picture works well for the 1D-network (polymeric) case of *a*-Se, as well as a host of organic glasses such as polystyrene. The Zachariasen model (of which the Polk model is a variation for an *elemental* amorphous solid) applies to 3D-network tetrahedrally-coordinated inorganic glasses.[5]

It has been difficult to visualize the structure of glasses whose crystalline counterparts have 2D-network (layer) structures. This is because of the topological problem of trying to substantially disorder layers by folding or twisting. (Imagine a telephone book.) Some success has been achieved by models which are locally layerlike.[6] Another approach is to construct a model in which the layers are cut into ribbons and tangled (linguini-like) to produce the glass. In effect, this results in a structure that is essentially a 1D-network system, a variation of the Flory (spaghetti-like) picture. The Phillips models for *a*-As_2S_3 and *a*-GeS_2 are specific examples of this.[1] Such structures will be molecular solids because their network dimensionality is less than three.

Germanium disulfide is an important test case for the above contrasting models of topological disorder. In addition to the glass *a*-GeS_2, this compound occurs in two crystalline forms which have different network dimensionalities. The high-temperature polymorph is a 2D-network layer crystal.[7] This form will hereafter be designated 2D-GeS_2. A single layer is represented in Fig. 2. (Ignore the dashed lines for the present.) 2D-GeS_2 consists of chains of corner-linked $Ge(S_{1/2})_4$ tetrahedra, cross-linked by edge-sharing tetrahedra to form a 2D network. The presence of edge-sharing tetrahedra means that there are pairs of Ge atoms that are connected by *two* S bridges. The varied linking produces both six- and four-membered rings in a 2:1 ratio. The low-temperature polymorph of *c*-GeS_2 is a complicated 3D-network structure.[8] It will be designated 3D-GeS_2. A model of this structure is reproduced in Fig. 3.[1] For 3D-GeS_2 the smallest ring unit is six-membered, and, as in SiO_2, there are no edge-sharing tetrahedra. 3D-GeS_2 is notable for containing rather large hollow volumes surrounded by 24 $Ge(S_{1/2})_4$ corner-sharing tetrahedra. Phillips[1] asserts that the difference between 2D-GeS_2 and 3D-GeS_2 is actually subtle. For both materials the

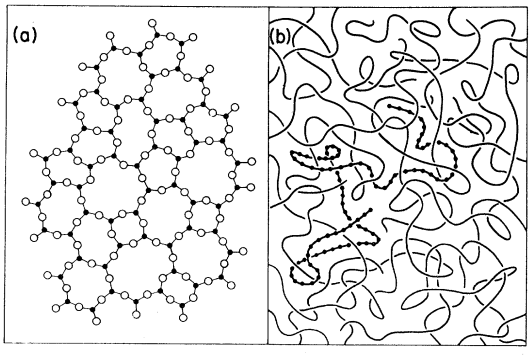

FIG. 1. Two canonical models for amorphous solids containing covalent networks: (a) Zachariasen continuous random network (e.g., *a*-Ge, *a*-SiO_2), (b) Flory random-coil polymer model (e.g., *a*-Se, polystyrene).

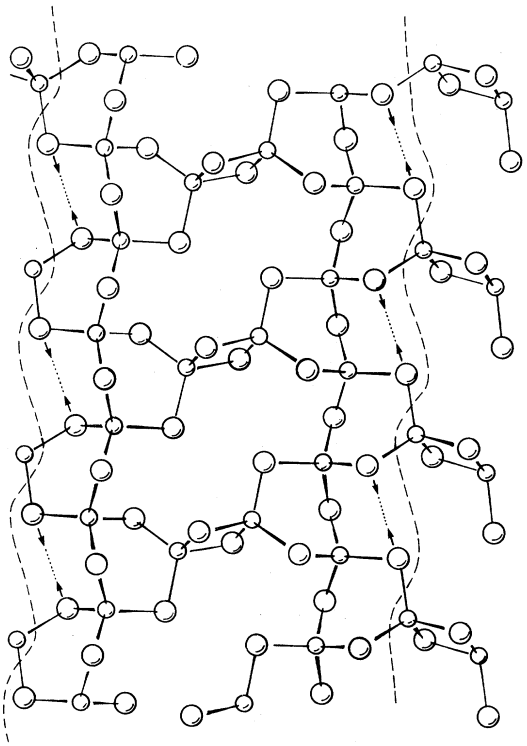

FIG. 2. Structure of a single layer of 2D-GeS_2. Note the edge-linked tetrahedra forming four-membered rings with two —S— bridges connecting a single pair of Ge atoms. In Phillips's model (Ref. 1) for *a*-GeS_2, linguini-like structural units are formed by breaking Ge—S bonds along the dashed lines and reconstructing S—S bonds along the dotted lines.

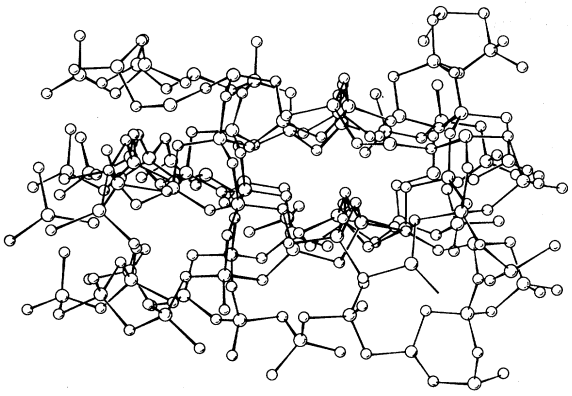

FIG. 3. Structure of 3D-GeS_2 (after Ref. 1) showing the large ellipsoidal hollows.

internal surfaces (whether layer or hollow) contain only chalcogen atoms. The topological difference derives from the radius of curvature of these internal surfaces, which is infinite (open surfaces) for 2D-GeS_2, but finite (closed surfaces) for 3D-GeS_2.

The goal of our study is to experimentally probe the network dimensionality of a-GeS_2 by comparing the results of high-pressure optical experiments carried out on *all three forms* of GeS_2. Compression distinguishes between molecular and nonmolecular solids. This is due to the large bonding-strength dichotomy between inter- and intra-molecular bonds in molecular solids. For (<3D)-network materials, compression mainly forces the molecular units closer together without affecting nearest-neighbor distances; for 3D-network solids, compression does substantially decrease the nearest-neighbor separation. It has been demonstrated that this basic difference manifests itself in several optical properties. The fundamental absorption edge in molecular insulators redshifts strongly to lower energy with increasing pressure, whereas the edge in 3D-network Ge-family materials generally exhibits a strong blue shift.[9–12] The refractive index of molecular solids increases strongly with pressure, while the index for Ge-family materials decreases.[13–15] This photoelastic distinction has proven to be a particularly useful indicator of network topology because it reveals differences in the behavior of an appropriately defined average gap.[15] Finally, the Gruneisen γ's for Raman-active phonons in molecular solids scale over two orders of magnitude as ν^{-2}, whereas the analogous γ's for 3D-network Ge-family materials are of order unity.[16–18]

The present article deals with the effects of compression on the electronic optical properties, namely the absorption edge and refractive index, of the three forms of GeS_2. High-pressure Raman measurements of phonons in these materials will be the subject of a future paper.[19]

No pressure-optical studies for any of the GeS_2 forms have been reported in the literature. At atmospheric pressure, absorption-edge[20–22] and refractive-index[20,23] measurements have been reported for 2D-GeS_2 and a-GeS_2. (References 22 and 23 pertain to the glass.) The optical properties of 3D-GeS_2 have not been previously investigated at any pressure. Section II of this paper details our measurement techniques, and Sec. III presents the experimental results. In Sec. IV we discuss these results in relation to the network dimensionality and medium-range order of a-GeS_2. Section V presents a summary of the important points.

II. EXPERIMENT

Our measurements were performed with an optical diamond-anvil press, in conjunction with a projection microscope and monochromator system. The diamond-anvil press was of the National Bureau of Standards design; it was used in the gasketed configuration, with 4:1 methanol:ethanol solution as the pressure-transmitting medium.[24] This fluid remains hydrostatic until its glass-transition pressure, which is ~ 95 kbar under the room-temperature conditions of these experiments. Pressure was determined in the sample chamber by simultaneously loading a chip of ruby with the sample and measuring the R_1 and R_2 luminescence peaks. The calibrated shift of these peaks with pressure has become a widely accepted secondary standard to ~ 1 Mbar.[25] Nonhydrostatic conditions appear as a broadening of the R_1 and R_2 lines for pressures greater than 95 kbar. The diamond anvils (arranged in the Bridgman opposed-anvil configuration) also serve as optical windows to the pressure chamber.

The cell was mounted on the X-Y micrometer stage of a projection microscope with standard glass lens optics giving magnifications in the range $\times 25 - \times 50$. The approximate sample area within the 250-μm-diameter pressure chamber (gasket hole) was 75×75 μm^2. The projected image of the sample (or ruby) was focused onto a variable diameter aperture. This aperture was then closed down to mask out background light from around the sample. However, a residual background remains due to unfocused scattered light generated in the diamond cell and microscope optics. This back-

ground limited our detection capability at high pressure to transmissions $I/I_0 > 10^{-2}$, and the corresponding cutoff of the glass optics restricted us to energies below 3.5 eV. However, the $P=0$ (1 atm) measurements shown in Figs. 3—5 were performed outside the diamond cell using a system with all-reflecting optics which gave considerably better scattered-light rejection and uv capability; in this case the detection limit was $I/I_0 > 10^{-4}$. We have not attempted to compensate for refractive index changes in the alcohol medium or the diamonds.

The 2D-GeS_2 samples used in these experiments were provided by Z. V. Popovic of Belgrade University. The method of growth (see Ref. 20) was similar to that described below. Stoichiometric bulk a-GeS_2 was synthesized from the high-purity elements in evacuated silica ampoules, during which time the sample was melted and rapidly cooled to form a glass. For the crystal growth experiments that yielded our 3D-GeS_2 samples, charge material was obtained by subsequently crystallizing the glass to ensure that the ingot was homogeneous, any S deficiency being evident from dark-colored GeS; transparent GeS_2 was then selected. Crystal growth consisted of sublimation in evacuated silica ampoules, into which GeS_2 charge material and ~ 0.1 at. % excess S were added. The two different polymorphs could be separately obtained under nearly isothermal vapor transport conditions at 800 °C, whereas an intergrown mixture of platelets (2D-GeS_2) and rods (3D-GeS_2) were obtained by transport from a charge temperature of 800 °C to a growth temperature ~ 600 °C. The latter condition, with the large temperature gradient, produced much faster growth rates. However, it is unclear whether the growth temperature or the secondary nucleation are necessary or sufficient conditions for obtaining the different polymorphs of GeS_2.

The three GeS_2 forms were identified by x-ray[26] and Raman[19] measurements, as well as by their morphology. Under $\times 50$ magnification the layer-morphology of 2D-GeS_2 was apparent from the several platelets that made up each sample. In contrast the 3D-GeS_2 samples were comprised of rods. For the crystalline forms, cell constants could not be determined in a routine fashion, because the samples were multicrystalline. However, since the polymorphic forms were known to be either the high-temperature layer structure or the low-temperature 3D-network type,[7,8] a powder pattern of each structure was calculated. The 2θ values so obtained were compared with measured 2θ values by computer centering of 25 random reflections for each sample. This procedure clearly separated the 2D- and 3D-GeS_2 varieties. The a-GeS_2 material displayed the characteristic diffuse diffraction pattern. The different sharp-line Raman spectra of the two crystalline forms could be easily distinguished from each other and from the broad-band spectrum of the glass.[19]

Cleaved samples of the crystal forms and polished wafers of GeS_2 glass were used. The optical surfaces were of sufficient quality to give distinct interference fringes in the transparent region (see Figs. 4—6). It was always possible to observe ~ 5—15 μm diameter areas of the samples that

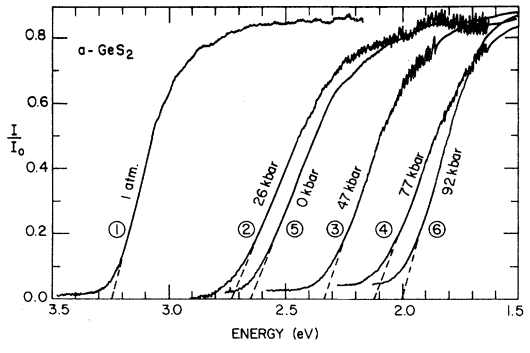

FIG. 4. Pressure-induced red shift of the a-GeS_2 absorption edge. Transmission is plotted against photon energy increasing to the left. Circled numbers give the data-recording sequence. Edge position E_t was determined by the extrapolated (dashed line) zero-baseline crossing. Interference fringes used to measure the near-infrared refractive index are also shown for some pressures (see discussion in text).

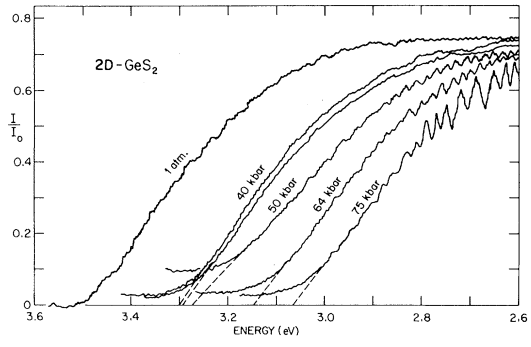

FIG. 5. Pressure-induced red shift of the 2D-GeS_2 absorption edge. Note the reduced span of the energy scale with respect to Fig. 4. For further details see text and Fig. 4.

were uniform and free from inclusions under $\times 50$ magnificaton. The optical path length through the sample was determined from the fringe spacing according to (Ref. 27) $nl = 0.620 dm/dE$. Here n is the refractive index for the appropriate polarization transverse to the direction of propagation within the sample, l is the sample thickness in microns parallel to the propagation direction, E is the photon energy in eV, and m is the fringe number. Our procedure was to plot m versus E over the measured range and to select a portion of this plot far enough into the transparent regime to show no discernible curvature over a span of $\sim$ 20 fringes. The slope of this linear portion was then determined from a least-squares fit. Since the maximum uncertainty in fringe position was $\pm$ 0.2 fringes, the estimated error in nl is $\pm$ 2%. The initial ($P = 0$) sample thicknesses were determined by this method using independent refractive index data,[20,23] and/or from direct measurement with a calibrated microscope. These thicknesses were 21 μm for a-GeS_2, 9 μm for 2D-GeS_2, and 25 μm for 3D-GeS_2, corresponding to n values of 2.2,[23] 2.6,[20] and 2.0, respectively.

To determine the band-gap pressure coefficients in a consistent manner, we extrapolated the linear portion of the measured transmission edges to the "zero" baseline (see Figs. 4—6). Given the thicknesses of our samples, and estimating that the baseline corresponds to $I/I_0 \approx 10^{-3}$, the energies so defined correspond to α values in the range $(3-7)\times 10^3$ cm^{-1}. We believe that the pressure coefficients of the actual electronic thresholds correspond closely to the shift of the energies defined by this extrapolation scheme because there is little change in shape of the transmission edges with pressure. Based on the variation in repeated measurements, the estimated uncertainty in these energies is $\pm$ (0.02 — 0.05) eV.

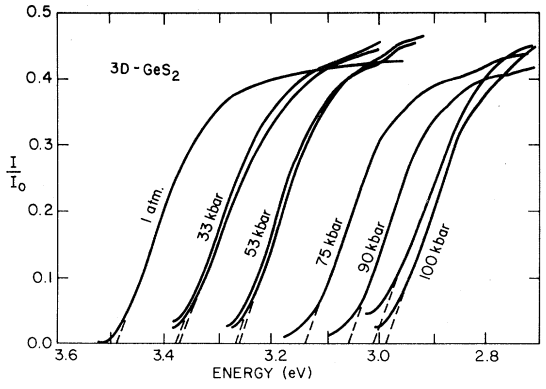

FIG. 6. Pressure-induced red shift of the 3D-GeS_2 absorption edge. Again, note the reduced range of the energy scale relative to Fig. 4. Data has been smoothed to suppress both noise and interference fringes. Details as in Fig. 4 and text.

III. RESULTS

Compression caused the absorption edge to shift to *lower* energy for each variety of GeS_2. However, the magnitude of this red shift is quite different among the three forms. Figures 4—6 display the measured transmission edges of a-GeS_2 (Ref. 28) 2D-GeS_2, and 3D-GeS_2 at various pressures. The different red shifts are quite apparent; they are roughly 1.3, 0.75, and 0.5 eV in 100 kbar for the amorphous, 2D, and 3D forms, respectively. The shift for a-GeS_2 is among the largest observed for the absorption edge of any semiconductor; it is sufficient to change the color of the sample from clear to deep red by 100 kbar.

Some details of these spectra are worth emphasizing. The interference fringes used to measure the refractive index have been retained on several of the curves for a-GeS_2 and 2D-GeS_2 (Figs. 4 and 5); for 3D-GeS_2 (Fig. 6) the spectra have been smoothed so that the fringes as well as the noise have been averaged in the displayed curves. Typical uncertainties in edge position are reflected in the duplicate measurements at 33, 55, and 100 kbar in Fig. 6, and 40 kbar in Fig. 5. These variations arise mostly from small and unsystematic changes in edge shape. They are typical also of sample-to-sample variations within a given GeS_2 form. (Three samples of a-GeS_2, three of 2D-GeS_2, and two of 3D-GeS_2 were measured.) The variations are inconsequential on the scale of the red shifts generated at the high pressures of our experiments. Over the restricted absorption range covered for each edge in Figs. 4—6, the steepness of each edge is seen to be relatively unaffected by pressure. The edge sharpnesses for the three materials (when corrected for differences in sample thickness) are not very different, with the 3D-GeS_2 edge being the sharpest. Note that the energy scale used in Fig. 4 for a-GeS_2 is much more extended than the scales used in Figs. 5 and 6. As mentioned in Sec. II, the $P = 0$ spectra were measured with the sample outside the diamond cell, using reflecting optics. This allowed us to probe the near-uv high-absorption tail of the $P = 0$ edges, which were near the 3.5 eV cutoff of our

microscope optics for 2D- and 3D-GeS_2. At $P=0$ the electronic threshold energies E_t (obtained by extropolation to the baseline) are 3.24 ± 0.05 eV, 3.48 ± 0.03 eV, and 3.49 ± 0.02 eV for a-GeS_2, 2D-GeS_2, and 3D-GeS_2, respectively. The first two values agree well with the existing $P=0$ results for a-GeS_2 (Ref. 22) and 2D-GeS_2.[20,21]

For a-GeS_2 (Fig. 4), the circled numbers labeling the spectra give the sequence in which the measurements were recorded. After steadily increasing the pressure to 77 kbar, the pressure was rapidly (~ 20 min) lowered to 0 kbar, held there for 18 h, and then rapidly raised to 92 kbar. This sequence revealed a large hysteresis in the edge shift. After quenching from 77 to 0 kbar, the edge returned only about halfway to its initial position. However, after 18 h at 0 kbar, a further shift to higher energy was observed (see Fig. 7). This behavior was typical of all a-GeS_2 samples measured, but the detailed hysteresis depended on the sample pressure history. This type of behavior has been found by the authors previously in a-As_2S_3,[11] and is evidently a manifestation of density relaxation in the glass after compression. One expects that the relaxation time would decrease with increasing temperature approaching the glass transition temperature.[29] We did not pursue this aspect in the present work. No similar hysteresis was observed for the crystals.

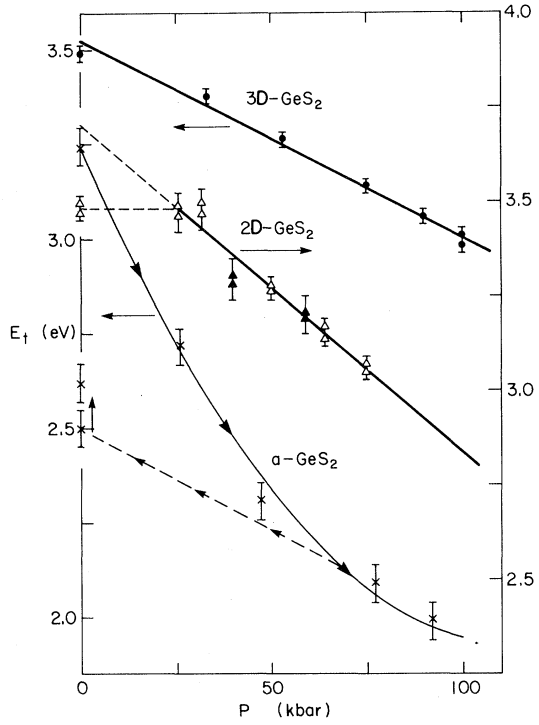

FIG. 7. Quantitative comparison of the pressure dependences of the absorption-edge positions for the three forms of GeS_2. The right-hand scale pertains to 2D-GeS_2 and the left-hand scale to a- and 3D-GeS_2. Solid curves are least-squares fits to the data. Dashed line and arrows for a-GeS_2 show hysteresis and recording sequence. Dashed lines for 2D-GeS_2 represent two options for the pressure-induced shift between 0 and 25 kbar.

The electronic threshold energy E_t is plotted as a function of pressure in Fig. 7 for the three GeS_2 forms. Least-squares fits to the data yield values for the initial ($P=0$) slopes of $-(23\pm4)$, $-(9\pm2)$, $-(5\pm1)$, in units of meV/kbar for a-, 2D-, and 3D-GeS_2, respectively. A rather large quadratic component of the shift is evident at high pressure for a-GeS_2, but not for the crystals.

Two sets of dashed lines appear in Fig. 7. For a-GeS_2 the dashed line indicates the nonreversible return of the edge to higher energy after quenching the pressure to 0 kbar from 77 kbar, and then waiting for 18 h at 0 kbar. Subsequent compression to 92 kbar red-shifted the edge to its estimated position at this pressure on the initial (solid) curve. For 2D-GeS_2, the dashed lines represent two possible scenarios for $P<30$ kbar. This ambiguity arises because the uv cutoff of our microscope did not permit us to follow the pressure dependence of an edge above 3.5 eV. Thus, the unchanged position of the edge at 1 atm, 26 kbar, and 32 kbar indicates either a rather strange nonlinear shift or a pressure-induced crossing of the lowest gap by an initially higher gap. By extrapolating the best-fit line for $P>26$ kbar to $P=0$, we find 3.7 eV for the initial position of this higher gap. A similar situation has been observed in trigonal Se, where the red shift of the indirect (lowest) absorption edge is only half that of the first reflectivity maximum associated with the lowest direct gap.[30] At this time we make no speculation as to the identities of the 3.5- and 3.7-eV gaps in 2D-GeS_2.

Analysis of our data for the pressure dependence of the interference-fringe spacings reveals that compression causes the refractive indices of all three materials to increase; however, the magnitude of the effect is much smaller for 3D-GeS_2 than for the two other forms. The behavior is illustrated in Fig. 8, where the optical path length nl (normalized by its $P=0$ value) is plotted against pressure. It is apparent that the increase in nl for a-GeS_2 and 2D-GeS_2 is essentially the same, approximately 20% in 100 kbar. By contrast, for 3D-GeS_2 the increase is about an order of magnitude smaller.

To describe the compression-induced variation in

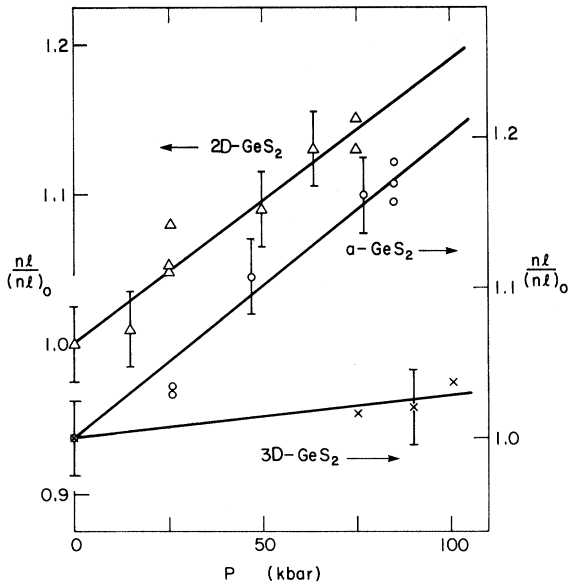

FIG. 8. Quantitative comparison of the effect of pressure on the near-infrared optical path lengths nl of the three GeS_2 forms. Right-hand scale pertains to a- and 3D-GeS_2; left-hand scale pertains to 2D-GeS_2. Solid lines are least-square fits to the data; the slopes give $[(d\ln n/dP)-(K/3)]$. Note the similar slopes for a- and 2D-GeS_2.

n, i.e., the photoelastic response, we shall employ the coefficient χ'. This is the Grüneisen-parameter analog for the electronic susceptibility. It is defined by[15]

$$\chi' = -\frac{d\ln\chi}{d\ln V} = \frac{n^2}{(n^2-1)}\frac{2}{K}\frac{d\ln n}{dP}\ , \tag{1}$$

where $\chi=(\epsilon_0-1)/4\pi$, $\epsilon_0=n^2$, n is the infrared (intermediate between phonon and electron excitations) refractive index, and K is the compressibility. Equation (1) must be evaluated at $P=0$.

In order to determine χ' from our measurements, K must be known. Unfortunately, there are no compressibility data in the literature for any of the GeS_2 forms. Consequently, we have estimated K by an empirical rule which has been shown to hold for families of related crystalline and amorphous solids (e.g., for the As-Se system).[31] This rule relates the average volume compressibilities $K(1)$ and $K(2)$ of two materials by

$$\frac{K(1)}{K(2)} = \left[\frac{\rho_{\rm mol}(2)}{\rho_{\rm mol}(1)}\right]^4\ , \tag{2}$$

where $\rho_{\rm mol}(i)$ is the mean molecular density of material i. K values for the three GeS_2 forms were obtained by scaling $K(a\text{-Se})$ according to this rule.[15,31] The K values are 7.4×10^{-3} kbar^{-1}, 5.6×10^{-3} kbar^{-1}, and 4.9×10^{-3} kbar^{-1} for a- , 2D- , and 3D-GeS_2, respectively. These estimated compressibilities seem quite reasonable.

The solid lines in Fig. 8 are the least-square fits to the data. Their slopes, which give directly $[(d\ln n/dP)-(K/3)]$, are $(2.1\pm0.4)\times10^{-3}$ kbar^{-1}, $(1.9\pm0.4)\times10^{-3}$ kbar^{-1}, and $(0.3\pm0.4)\times10^{-3}$ kbar^{-1}, for a- , 2D- , and 3D-GeS_2, respectively. The corresponding χ' values are 1.5, 1.6, and 1.0 with experimental uncertainty in the range 10–20%.[15] For the reader's convenience, all of the preceding numerical results are summarized in Table I.

For 3D-GeS_2, a phase transition was observed at 110 ± 5 kbar. At this pressure the sample color changed abruptly from clear (at 100 kbar the edge was at 3.0 eV, see Fig. 7) to brown, implying an associated red shift of $\sim$ 1.0 eV. It was possible to stop the transition before all the material had transformed, so that separate measurements on the coexisting phases could be performed. The absorp-

TABLE I. Summary of numerical results for the present study. Values in parentheses are estimated according to text.

Material	a-GeS_2	2D-GeS_2	3D-GeS_2
E_t (eV)	3.24±0.05	3.48±0.03 (3.7)	3.49±0.02
dE_t/dP (in meV/kbar)	−23 ±4	−9 ±2	−5 ±1
$d\ln n/dP$ (in 10^{-3} kbar^{-1})	4.6 ±0.4	3.8 ±0.4	1.9 ±0.4
χ'	1.5 ±0.15	1.6 ±0.15	1.0 ±0.2
n	2.2[a]	2.6[b]	2.0
K (in 10^{-3} kbar^{-1})	(7.4)	(5.6)	(4.9)

[a]Reference 23.
[b]Reference 20.

tion edge of the transformed region was very broad, and there was visual evidence of fracture and crumbling. The absorption edge of the unchanged region appeared normal. Raman spectra of the high-pressure phase were recorded and found to be substantially different from the low-pressure phase.[19] After quenching to $P=0$, visual observation and Raman measurements indicated that the new phase was retained. No transitions were observed for either a-GeS_2 or 2D-GeS_2, but in these cases the maximum applied pressures were 95 and 82 kbar, respectively.

Before going on with the detailed interpretation, we call attention to another aspect of these results that is particular to 3D-GeS_2. For this material the effects of pressure on both the edge and index are somewhat anomalous. They do not fit the pattern of other covalent 3D-network solids. For example, the Ge-family (groups IV, III-V, and II-VI) semiconductors generally exhibit a strong pressure-induced increase in the lowest band gap (or an extremely weak decrease for the $\Gamma-X$ indirect gap) and a decrease in n. On the other hand, the observed edge red shift and increase in n for 3D-GeS_2 are rather small compared to the typical behavior of ($<$3D)-network molecular solids, and also compared to the response of a- and 2D-GeS_2.

IV. IMPLICATIONS FOR THE NETWORK DIMENSIONALITY OF GeS_2 GLASS

Our interpretation of the preceding results is based on the severe dichotomy between the strength of intermolecular and intramolecular forces in molecular solids, as opposed to 3D-network materials. Consider the Ge-family semiconductors as a prototype example of the latter group. Because of their isotropic 3D-network, a macroscopic compression ΔV is *fully* transferred to nearest-neighbor bond reduction Δa, according to $\Delta V/V=3\Delta a/a$. This is not the case for low-network dimensionality ($<$3D) solids. Under compression their molecular (viz. network) units simply move closer together without substantially affecting the nearest-neighbor separation. In essence, the stiff nearest-neighbor bonds that form the covalent ($<$3D) network are insulated from compression by the soft intermolecular (i.e., internetwork) forces. The latter bear the brunt of the macroscopic volume change.

A qualitative explanation for the effects of pressure on the electronic properties of structures having different network dimensionality (viz. molecular versus nonmolecular) was given by Zallen and Blossey.[10] According to this picture, the pressure-induced bond-length reduction in 3D-network (e.g., Ge-family) solids causes an increase in the *average* bonding-antibonding gap, and the lowest gap generally follows suit.[12] Thus, the absorption edge should blue-shift, as is typically observed for Ge-family semiconductors. Furthermore, the larger bonding-antibonding gap accounts for the decreased refractive index, according to any of the single-oscillator dielectric models.[14,32] In contrast to this, the bonding-antibonding interaction is not substantially affected by pressure in ($<$3D)-network solids. Instead, the electronic bands in molecular semiconductors are expected to broaden because the intermolecular overlap increases strongly as the molecular (i.e., covalent-network) units crowd closer together. This explains the red shift of the absorption edge. One might also argue that the refractive index should increase as the electronic threshold is reduced. However, it has been shown that a more detailed interpretation, based on a two-oscillator model, is needed to explain the observed photoelastic behavior.[15]

Based on these remarks, the strong red shift of the a-GeS_2 edge (Figs. 4 and 7) is evidence for the molecular character, the ($<$3D)-network topology, of this glass. We may compare the -23 meV/kbar coefficient for the edge of a-GeS_2 to the analogous coefficients of other known molecular chalcogenides: -23 meV/kbar (Refs. 30 and 33) and -17 meV/kbar (Refs. 34 and 35) for c- and a-Se, -20 meV/kbar (Ref. 36) for c-Te, -14 meV/kbar (Ref. 37) and -18 meV/kbar (Ref. 11) for c- and a-As_2S_3, and -15 meV/kbar (Refs. 13, 38, and 39) for both c- and a-As_2Se_3. Clearly a-GeS_2 falls into this pattern, with the amount of overlap-induced band broadening approximately the same as for the cited molecular chalcogenides. The fact that the red shift for a-GeS_2 is actually larger than for the bona fide 2D-network layer crystal 2D-GeS_2 (see Fig. 7) only lends further support to the ($<$3D)-network molecular model of the glass.

The red shift of the 3D-GeS_2 edge is difficult to understand. A blue shift had been anticipated because of the formal 3D-network structure. However, in crystals it is known that the pressure coefficients of interband transitions associated with specific critical points can vary. For example, in Ge-family crystals the indirect $\Gamma-X$ edge also has a negative coefficient.[12] A more intriguing possibility is that the red shift for 3D-GeS_2 is evidence

for the subtle structural difference between the 2D- and 3D-crystalline varieties suggested by Phillips.[1] The latter viewpoint is also supported by our refractive index data, and will be discussed further below.

The photoelastic response, because it reflects the average behavior of the electronic bands, is a more revealing measure of network topology than the shift of the electronic threshold. Weinstein *et al.*[15] have demonstrated a substantial correlation between the sign and magnitude of χ' [see Eq. (1)] and network dimensionality. Covalent 3D-network semiconductors of the Ge family, whether crystalline or amorphous, invariably have $\chi' < 0$, reflecting negative dn/dP. In contrast, chalcogenide-based molecular crystals and glasses, with ($<$3D)-network dimensionality, exhibit $\chi' > 1$, reflecting large positive dn/dP. (Note that $\chi' = 1$ is the pure volume-change contribution, obtained if electron energy and wave function changes are negligible.)

This correlation is best displayed in the graph of χ' versus $2\eta/E_g$ first introduced in Ref. 15 and shown in Fig. 9. Here E_g is the Penn-Phillips gap[40]; it is determined solely by the refractive index and the effective valence-electron density. η is an experimentally determined dimensionless scaling factor of order unity. (For Ge-family solids $\eta \equiv 1$.) Two separate linear trends are exhibited in Fig. 9, one for $\chi' < 0$ Ge-family materials and the other for $\chi' > 1$ molecular chalcogenides. These linear dependences have been explained using a model that approximates the dielectric response of Ge-family solids and molecular chalcogenides by one and two oscillators (of the Penn-Phillips type), respectively.[15] The utility of the two-oscillator model for chalcogenides rests on the experimental dielectric loss spectra, which generally show two distinct structures in the valence electron region. [See, for example, *c*-, *a*-$GeSe_2$ (Ref. 41) or *c*-, *a*-Se, Te, As_2S_3, and As_2Se_3 (Ref. 42.)] In chalcogenides it is reasonable to associate the two oscillators mainly with nonbonding-antibonding (oscillator I) and bonding-antibonding (oscillator II, at higher energy) transitions.[43] The band width enters the model through η, which depends on the energy separation between the two oscillators.

For the present work, the essential features of this model are as follows[15]: $\chi' < 0$ reflects domination of the photoelastic response by a single *increasing* bonding-antibonding gap; $\chi' > 1$ reflects a photoelastic behavior dominated by the *decreasing* nonbonding-antibonding gap and uninfluenced by the *stationary* bonding-antibonding gap. For the latter molecular-solid case, the expected pressure-induced band broadening is manifest through the increased separation of the two oscillators, whereas the anticipated insensitivity of the nearest-neighbor distance to compression is reflected in the unchanged bonding-antibonding energy.

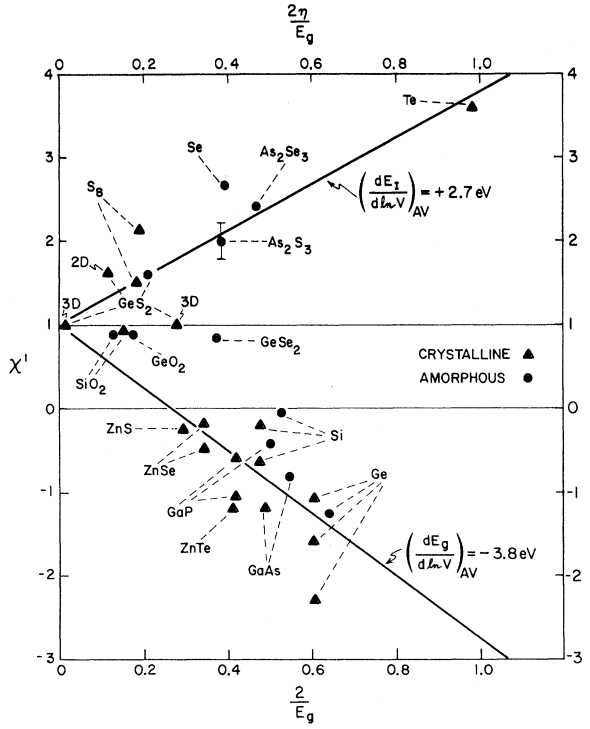

FIG. 9. Photoelastic-response—network-dimensionality correlation diagram introduced in Ref. 15. χ' is the Gruneisen-parameter analog of the electronic susceptibility [Eq. (1)], E_g is the Penn gap, and η is a dimensionless scaling parameter dependent on band width. $\eta \equiv 1$ for Ge-family (single oscillator) materials. The plot divides into three regions: $\chi' < 0$ pertains to 3D-network Ge-family solids, $\chi' > 1$ pertains to ($<$3D)-network molecular chalcogenides, and $0 \leq \chi' \leq 1$ is an ambiguous region. 3D-GeS_2, on the $\chi' = 1$ borderline, is plotted twice for $\eta = 1$ and η given by Eq. (8) of Ref. 15.

Figure 9 shows that the χ' values of *a*-GeS_2 and 2D-GeS_2, 1.5 and 1.6, respectively, are quite similar. According to the model of Ref. 15, this is due to similar pressure shifts for the appropriate average gap in each solid. More importantly, both materials fall well within the $\chi' > 1$ molecular solid region. The latter result was, of course, expected for the layer crystal 2D-GeS_2. Its occurrence for *a*-GeS_2, considered together with the red shift of the edge, argues strongly for ($<$3D)-network topology in this glass. If, to the contrary, a 3D-network structure were present, compression would decrease

the nearest-neighbor distance (Ge—S covalent bond length), which in turn would increase the bonding-antibonding gap. This would make a negative contribution to χ', decreasing it to $\chi' \approx 1.0$ as for 3D-GeS_2 (note also the χ' values of *c*-, *a*-SiO_2), or even making it negative as for Ge-family solids. Since this is clearly not the case, we conclude that the χ' value for *a*-GeS_2 can be explained in a manner similar to that for other known molecular chalcogenides (e.g., besides 2D-GeS_2, see in Fig. 9 *a*-As_2S_3, *a*-As_2Se_3, *a*-Se, *c*-Te.) As a consequence of low-network dimensionality, the electronic response to pressure of *a*-GeS_2 is dominated by increased overlap between nonbonding electrons located within a highly compressible *intermolecular* volume. This makes a large positive contribution to χ', increasing its value to $\chi' > 1$.

The photoelastic response of 3D-GeS_2 appears to be a borderline case. The refractive index increases weakly with pressure, unlike 3D-network Ge-family solids; however, the observed χ' value lies on the boundary of the molecular solid region at $\chi' = 1.0$. This result, along with the unexpected red shift of the electronic threshold, raises an interesting possibility: With respect to certain properties 3D-GeS_2, may resemble the molecular solid 2D-GeS_2 more closely than its formal network topology would lead one to expect. This curious hybrid behavior could be related to the large ellipsoidal hollows in the 3D-GeS_2 structure (Fig. 3).[1] These voids are locally soft regions bounded by internal surfaces containing only chalcogenide atoms. Such a structure may permit 3D-GeS_2 to accommodate compression, at least in part, by bond bending (picture an accordionlike motion) rather than by bond shortening. This would partially insulate the covalent bond length from the effects of compression and attenuate the pressure-induced blue shift of the bonding-antibonding gap. Moreover, compression of the hollows will increase the lone-pair overlap of the chalcogens on facing surfaces, thereby producing a red shift of the nonbonding-antibonding gap. These two opposite contributions to χ' could easily explain the $\chi' = 1$ result. These considerations suggest that the special structure of 3D-GeS_2 tends to blur the distinction, with respect to the pressure dependence of its electronic properties, between this particular 3D-network chalcogenide and the molecular chalcogenides.

It is interesting to speculate that the phase transition seen at 110 kbar for 3D-GeS_2 could correspond to some discontinuous distortion or collapse of the hollows. Recently, evidence for similar distortions of voids in *a*-Si:H has been observed in high-pressure luminescence studies.[44]

The primary conclusion of this study is that *a*-GeS_2 is *not* a 3D-network glass akin to its chemical cousin *a*-SiO_2 (as conventional wisdom has maintained), but instead is a molecular glass with ($<$3D)-network topology. Referring back to Fig. 1 our results favor a Flory model of the structure (1D-network polymeric glass) over a Zachariasen model (continuous 3D-network glass). This conclusion is consistent with a class[6] of linguini-like models for structural disorder, of which Phillips's "partially polymerized cluster" model is an intriguing example. Phillips has proposed a specific structure for the "linguini" units of *a*-GeS_2.[1] Each unit can be formed from a single layer of 2D-GeS_2 in the manner indicated in Fig. 3: One cuts the layer along the dashed lines and reconstructs the edges with chalcogen-chalcogen bonds along the dotted lines. Although the present high-pressure experiments have enabled us to distinguish between 3D-network and ($<$3D)-network topology, they do not give us more detailed information as to what type of low-network-dimensionality structure applies. In particular, we cannot determine the width or the internal structure (including possible topological disorder) of each linguini unit. In a future article describing high-pressure Raman studies of the three GeS_2 forms, we hope to shed more light on these issues.[19]

V. SUMMARY

A series of experiments have been carried out to determine the sensitivity to pressure of the absorption edge and the near-infrared refractive index of three solid forms of germanium disulfide: the amorphous form *a*-GeS_2, the layer-structure crystalline form 2D-GeS_2, and the quartz-like crystalline form 3D-GeS_2. The main experimental findings are summarized in Figs. 7 and 8 and in Table I. For all three solids, the absorption edge redshifts under pressure. The rate of decrease of the electronic threshold is swiftest for the glass, slower for 2D-GeS_2, and slowest for 3D-GeS_2. The magnitude of the band-gap pressure coefficient observed for *a*-GeS_2 is among the largest known for any semiconductor. The refractive index of each of the three materials increases with compression: The sensitivity to pressure is similar for *a*-GeS_2 and 2D-GeS_2, but is significantly smaller for 3D-

GeS_2.

Exploiting the opportunity for a comparison of the behavior of the glass to that of two crystalline forms, one a 3D-network solid and one a molecular solid, and making use of a recently established correlation between covalent-network dimensionality and photoelastic response, we have been able to interpret our pressure-optical data in terms which narrow the range of permissible models for the structure of the glass. Our experiments provide definite evidence that a-GeS_2 is *not* a 3D-network glass akin to silica, but instead has lower network dimensionality — i.e., it is a molecular glass. Most telling in this regard is the similarity between the pressure dependence of the refractive index of the glass and that observed for 2D-GeS_2. Also, the dimensionless photoelastic-response parameter χ' [defined in Eq. (1)] for a-GeS_2 falls well within the molecular-solid regime of the photoelastic-response—network-dimensionality correlation diagram (Fig. 9). χ' for 2D-GeS_2 also falls, as expected, within this regime. For 3D-GeS_2, the position of χ' occupies a somewhat anomalous borderline position on the correlation diagram, for reasons which appear to be associated with the hollows that are prominent in this 3D-network structure.

Affirming that a-GeS_2 is a molecular glass contradicts the conventional view of this glass as a silica-like Zachariasen continuous-random 3D network, but is consistent with a class of (<3D)-network models such as the Flory random-coil model for 1D-network polymeric glasses The Phillips model is of this type.

[1]J. C. Phillips, J. Non-Cryst. Solids 43, 37 (1981); 34, 153 (1979).

[2]R. Zallen, in *Proceedings of the 12th International Conference on the Physics of Semiconductors, Stuttgart, 1974,* edited by M. H. Pilkuhn (Teubner, Stuttgart, 1974), p. 621; R. Zallen, *The Physics of Amorphous Solids* (Wiley, New York, in press).

[3]W. H. Zachariasen, J. Am. Chem. Soc. 54, 3841 (1932).

[4]P. J. Flory, J. Chem. Phys. 17, 303 (1949); Science 88, 1268 (1975).

[5]R. Zallen, in *Fluctuation Phenomena,* edited by E. W. Montroll and J. L. Lebowitz (North-Holland, Amsterdam, 1979), p. 177.

[6]P. C. Taylor, S. G. Bishop, D. L. Mitchell, and D. Treacy, in *Proceedings of the Fifth International Conference on Amorphous and Liquid Semiconductors,* edited by J. Stuke and W. Brenig (Taylor and Francis, London, 1974), p. 1267.

[7]G. Dittmar and H. Schafer, Acta Crystallogr. Sect. B 31, 2060 (1975).

[8]G. Dittmar and H. Schafer, Acta. Crystallogr. Sect. B 32, 1188 (1976).

[9]H. G. Drickamer, *Solid State Physics,* edited by F. Seitz and D. Turnbull (Academic, New York, 1965), Vol. 17, pp. 38—43.

[10]R. Zallen and D. F. Blossey, in *Optical and Electrical Properties of Compounds with Layered Structures,* edited by P. A. Lee (Reidel, Dordrecht, 1976), p. 231.

[11]B. A. Weinstein, R. Zallen, and M. L. Slade, J. Non-Cryst. Solids 35,36, 1255 (1980); J. M. Besson, J. Cernogora, M. L. Slade, B. A. Weinstein, and R. Zallen, Physica (Utrecht) 105B, 319 (1981).

[12]R. Zallen and W. Paul, Phys. Rev. 155, 703 (1967).

[13]M. Kastner, Phys. Rev. B 7, 5237 (1973).

[14]J. A. Van Vechten, Phys. Rev. 182, 891 (1969).

[15]B. A. Weinstein, R. Zallen, M. L. Slade, and A. deLozanne, Phys. Rev. B 24, 4652 (1981).

[16]R. Zallen, Phys. Rev. B 9, 4485 (1974); R. Zallen and M. L. Slade, *ibid.* 18, 5775 (1978).

[17]T. Chattopadhyay, C. Carlone, A. Jayaraman, and H. G. v. Schnering, Phys. Rev. B 23, 2471 (1981).

[18]B. A. Weinstein and G. J. Piermarini, Phys. Rev. B 12, 1172 (1975).

[19]M. L. Slade, R. Zallen, and B. A. Weinstein (unpublished).

[20]P. M. Nikolic and Z. V. Popovic, J. Phys. C 12, 1151 (1979).

[21]V. V. Sobolev and V. I. Doneckih, Izv. Akad. Nauk. 8, 688 (1972).

[22]Y. Kawamoto and S. Tsuchihashi, J. Am. Ceram. Soc. 54, 131 (1971).

[23]G. Lucovsky, J. P. deNeufville, and F.L. Galeener, Phys. Rev. B 9, 1591 (1974). The value $n=2.1$ of these authors seemed low compared to our own result $n=2.3$; the average value $n = 2.2$ has therefore been adopted.

[24]G. J. Piermarini and S. Block, Rev. Sci. Instrum. 46, 973 (1975).

[25]R. A. Forman, G. J. Piermarini, J. D. Barnett, and S. Block, Science 176, 284 (1972); H. K. Mao and P. M. Bell, Science 200, 1145 (1978).

[26]Measurements and analysis performed by R. Meisner and J. M. Troup, Molecular Structure Corp., 3304 Longmire Dr., College Station, Texas 77840.

[27]M. Cardona, W. Paul, and H. Brooks, J. Phys. Chem. Solids 8, 204 (1959).

[28]R. Zallen, B. A. Weinstein, and M. L. Slade, J. Phys. Paris (in press).

[29]P. W. Bridgman and I. Simon, J. Appl. Phys. 24, 405 (1953).

[30]M. Kastner and R. R. Forberg, Phys. Rev. Lett. 36,

740 (1976); J. D. Joannopoulos, Th. Starkloff, and M. Kastner, *ibid.* 38, 660 (1977); H. Wendel, R. M. Martin, and D. J. Chadi, *ibid.* 38, 656 (1977).

[31]N. Soga, M. Kunugi, and R. Ota, J. Phys. Chem. Solids 34, 2143 (1973).

[32]S. H. Wemple and M. DiDomenico, Jr., Phys. Rev. B. 3, 1338 (1971).

[33]V. Y. Krisciunas, M. P. Mikalkevicius, and A. Yu Shileika, Fiz. Tverd. Tela (Leningrad) 7, 2571 (1965) [Sov. Phys.—Solid State 7, 2080 (1966).]

[34]R. S. Caldwell and H. Y. Fan, Phys. Rev. 114, 664 (1959).

[35]W. Fuhs, P. Schlotter, and J. Stuke, Phys. Status Solidi B 57, 587 (1973).

[36]Yu. V. Kosichkin, in *The Physics of Selenium and Tellurium,* edited by E. Gerlach and P. Grosse (Springer, Berlin, 1979), p. 96.

[37]J. M. Besson, J. Cernogora, and R. Zallen, Phys. Rev. B 22, 3866 (1980).

[38]A. J. Grant and A. D. Yoffe, Solid State Commun. 8, 1919 (1970).

[39]B. T. Kolomiets and E. M. Raspopova, Fiz. Tekh. Poluprovodn. 4, 157 (1970) [Sov. Phys.—Semicond. 4, 124 (1970)].

[40]D. Penn, Phys. Rev. 128, 2093 (1962); J. C. Phillips, Rev. Mod. Phys. 49, 317 (1970).

[41]D. E. Aspnes, J. C. Phillips, K. L. Tai, and P. M. Bridenbaugh, Phys. Rev. B 23, 816 (1981).

[42]J. Stuke, J. Non-Cryst. Solids 4, 1 (1970); R. E. Drews, R. L. Emerald, M. L. Slade, and R. Zallen, Solid State Commun. 10, 293 (1972).

[43]M. Kastner, Phys. Rev. Lett. 28, 355 (1972); H. L. Althaus, G. Weiser, and S. Nagel, Phys. Status Solidi B 87, 117 (1978).

[44]B. A. Weinstein, Phys. Rev B 23, 787 (1981).